What day-ahead reserves are needed in electric grids with high levels of wind power?

Brandon Mauch[1], Jay Apt[1], Pedro M.S. Carvalho[2], and Paulina Jaramillo[1]

[1] Carnegie Mellon Electricity Industry Center, Carnegie Mellon University, 5000 Forbes Ave, Pittsburgh, PA 15213, USA
[2] DEEC, Instituto Superior Tecnico, Technical University of Lisbon, Av. Rovisco Pais 1, 1049-001 Lisbon, Portugal
E-mail: mauchb@gmail.com

Abstract

Day-ahead load and wind power forecasts provide useful information for operational decision making, but they are imperfect and forecast errors must be offset with operational reserves and balancing (real-time) energy. Procurement of these reserves is of great operational and financial importance in integrating large-scale wind power. We present a probabilistic method to determine net load forecast uncertainty for day-ahead wind and load forecasts. Our analysis uses data from two different electric grids in the U.S. with similar levels of installed wind capacity but with large differences in wind and load forecast accuracy, due to geographic characteristics. We demonstrate that the day-ahead capacity requirements can be computed based on forecasts of wind and load. For 95% day-ahead reliability, this required capacity ranges from 2,100 MW to 5,700 MW for ERCOT and 1,900 MW to 4,500 MW for MISO (with 10 GW of installed wind capacity), depending on the wind and load forecast values. We also show that for each MW of additional wind power capacity in ERCOT 0.16 to 0.30 MW of dispatchable capacity will be used to compensate wind uncertainty based on day-ahead forecasts. For MISO (with its more accurate forecasts), the requirement is 0.07 to 0.13 MW of dispatchable capacity for each MW of additional wind capacity.

1. Introduction

Wind power has experienced substantial growth over the past decade in the U.S. and in Europe. Installed capacity in the U.S. increased more than tenfold from 4.2 GW in 2001 to 60 GW in 2012 (AWEA, 2013). Electricity generated from wind in the U.S. accounted for under 0.2% of total electricity production in 2001, and now provides over 3% of total electrical energy (EIA, 2013). European installed wind capacity increased fivefold in the same time period, from 17.3 GW to 94 GW, and produces over 6% of the total electrical energy produced (Wilkes et al., 2012).

Current levels of wind capacity do not pose a large problem for grid operators in most regions, but future growth will require operational changes in order to ensure a reliable grid (Xie et al., 2011). Since wind power is not dispatchable, wind forecasts are used along with load forecasts to make operational decisions ranging from minutes to days in advance (Botterud et al., 2010). Because forecasts are not perfect, excess dispatchable generation capacity must be procured to ensure reliability in the operation of the grid. The Electric Reliability Council of Texas (ERCOT) includes net load (load minus wind) forecast uncertainty in its operational reserve procurement decisions. ERCOT procures operational reserve capacity equaling 95% of net load forecast errors[1] (ERCOT, 2012). The remaining uncertainty is covered with balancing energy procured in the spot market. The Midcontinent Independent System Operator (MISO), on the other hand, does not rely on operating reserves to correct forecast errors. Instead, it strives to ensure that adequate supply is available in the spot markets to handle forecast uncertainty. However, on a percentage of energy basis, MISO has less wind power than ERCOT (see table 1 below) and stronger transmission ties to neighboring grids.

The cost of balancing wind forecast uncertainty has been estimated in several studies. A review of the literature suggests the range of estimates is from $2.5 (Elektrotek, 2003) to $7 (EnerNex, 2007) per MWh of wind energy generated. Two important points should be made here. First, these estimates include the cost of balancing wind variability over time scales of seconds to minutes along with the costs

[1] Since ERCOT caps the amount of non-spinning reserves to 2000 MW, there are times when operational reserves is less than the 95th percentile of net load forecast errors.

of balancing longer time scale wind forecast errors. Second, wind forecast uncertainty is balanced with non-spinning reserves which are relatively slower and less costly than other forms of operating reserves such as regulation and spinning reserves. The analysis presented here does not consider economics of wind forecast error balancing.

The growth of wind power creates a need to update unit commitment and operating reserves procurement algorithms. Wang et al. (2008) proposed a model to incorporate the uncertainty of wind forecasts in unit commitments. Doherty and O'Malley (2005) presented a reserves procurement model that combines wind forecast uncertainty with load forecast uncertainty and generator forced outage probabilities. Ortega-Vazquez and Kirschen (2009) and Matos and Bessa (2009) each presented decision analytic frameworks to determine operating reserves in systems with wind power by balancing the cost of reserves and the cost of load curtailments. Bouffard and Galiana (2008) presented an economic dispatch algorithm that accounts for wind forecast uncertainty.

In the work cited above, wind and load forecast errors are generally modeled as normally distributed random variables. The one exception is Matos and Bessa, who used a non-parametric model for wind forecast errors. As shown by Hodge et al. (2012), wind forecast errors at the regional level are generally not Gaussian. Lange (2005) and Bludszuweit et al. (2008) demonstrated that wind forecast errors have distributions that can be highly skewed when the forecast is for a very low or high value of wind power. Wind forecasts near the middle of the forecast range have more symmetric error distributions (although not necessarily Gaussian). This is important in power system modeling as the representation of wind forecast uncertainty appears to have a significant effect on unit commitment results (Lowery and O'Malley, 2011).

Here we focus on net load forecast uncertainty as a function of the forecast quantity of wind generator output. At wind levels where net load uncertainty is dominated by wind forecast uncertainty, operational decisions should be based on a systematic assessment of net load uncertainty reflecting changes in wind forecast levels. Using data from ERCOT and MISO, we show that neither wind nor load forecast errors are normally distributed random variables, and describe the influence of load and wind forecast levels on

net load uncertainty. Finally, we estimate dispatchable generation requirements in grids with much higher wind power.

2. Wind and Load Data

We use data on wind and load forecasts along with actual values of wind and load from ERCOT and MISO. The ERCOT data consist of hourly wind forecast values for 1 to 48 hour look-ahead times covering 2009 and 2010. AWS Truepower provided actual wind generation values along with estimated uncurtailed wind generation potential. In order to analyze wind power uncertainty, we used estimated values of uncurtailed wind power to remove the effect of wind curtailments which are a result of real time operations and are not considered in wind power forecasts. AWS Truepower estimated hourly uncurtailed wind power values using measurements taken from wind farms in ERCOT and curtailment instructions issued by ERCOT. ERCOT curtailed an estimated 17% of wind generation in 2009 and 10% of wind generation in 2010 (Rogers et al., 2010). Day-ahead load forecasts were obtained from the Ventyx database.

MISO wind forecast data were obtained from their website, which provides day-ahead wind forecasts and actual wind generation. Our data span February 2011 to May 2012. Day-ahead load forecasts and observed loads were also obtained from the Ventyx database. Wind curtailments in MISO were estimated to range from 2% to 6% each month (MISO, 2012). Since the curtailments are small and we do not have hourly data on curtailment quantities, we neglect these curtailments in our analysis.

Table 1: Summary of wind and load in ERCOT and MISO during the time periods of the data we used in this study.

	ERCOT	MISO
Date Range	Jan 2009 – Dec 2010	Feb 2011 – May 2012
Average Load	36 GW	61 GW
Maximum Load	66 GW	104 GW
Average Nameplate Wind Capacity	8.8 GW	10 GW
Average Wind Capacity Factor[1]	0.35	0.33
Percentage of load served by wind[1]	8.7%	5.5%
Mean absolute wind forecast error (percentage of installed wind capacity)	11%	6.1%
Root mean squared wind forecast error (percentage of installed wind capacity)	14%	8.1%
Mean absolute forecast error (percentage of mean load)	3.1%	1.7%
Root mean squared load forecast error (percentage of mean load)	4.2%	2.2%

[1]For ERCOT, this neglects wind curtailments.

Aggregate wind power in MISO has a significantly lower forecast error than does ERCOT (table 1). During the time covered by our dataset, ERCOT and MISO had similar levels of installed wind capacity (~10 GW). However, the wind farms in MISO's territory span a much larger area than in ERCOT (figure 1). Large wind power footprints reduce the correlation of wind generation between wind farms, and lower variability in aggregate wind generation (Katzenstein et al., 2010; Fertig et al., 2012). The accuracy of wind forecasts improves as the variability decreases (Focken et al., 2002).

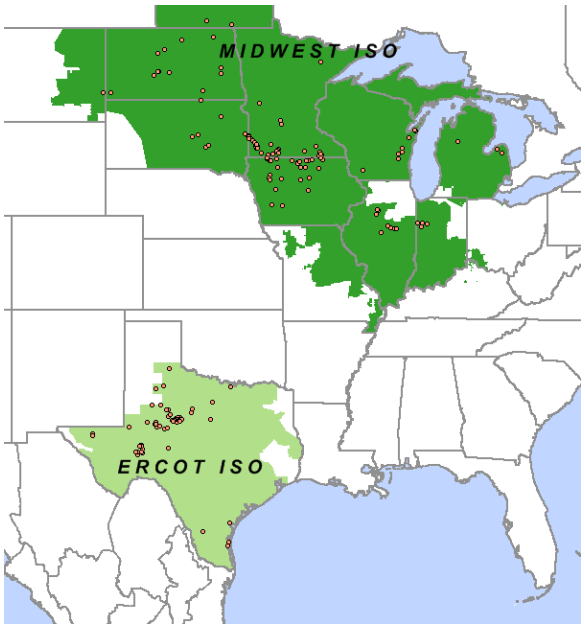

Figure 1: Map of wind farms in ERCOT and MISO. Data source: Ventyx.

3. Day-ahead uncertainty

3.1 Day-ahead load forecast uncertainty

The data in table 1 show that load forecasts tend to be more accurate than wind power forecasts. Operators compute load forecasts at many time intervals for daily operations. Here we are concerned with the forecasts made one day in advance, which are used to make decisions in unit commitment and operating reserve levels. Figure 2 shows actual hourly load versus forecasted load in ERCOT for one week in January. The bottom line in figure 2 illustrates the forecast error. We define the absolute forecast error as the forecast value minus the actual value.

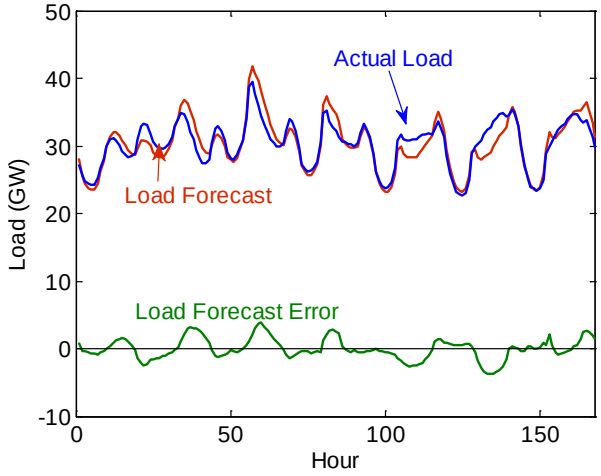

Figure 2: Forecasted load, actual load and load forecast errors in ERCOT for the week of February 28 – March 6, 2009.

The distribution of load forecast errors in both ERCOT and MISO is dependent on the load forecasts. Figure 3 shows the hourly load forecast errors plotted against the load forecasts. All data are normalized by the mean load in the respective grid. In our analysis we divided the load forecast data into three forecast bins as shown in figure 3: low load (forecasts less than 90% of mean load), medium load (between 90% and 120% of mean load) and high load (forecasts greater than 120% of mean load). We choose these bins to capture the range of variance of the forecast errors.

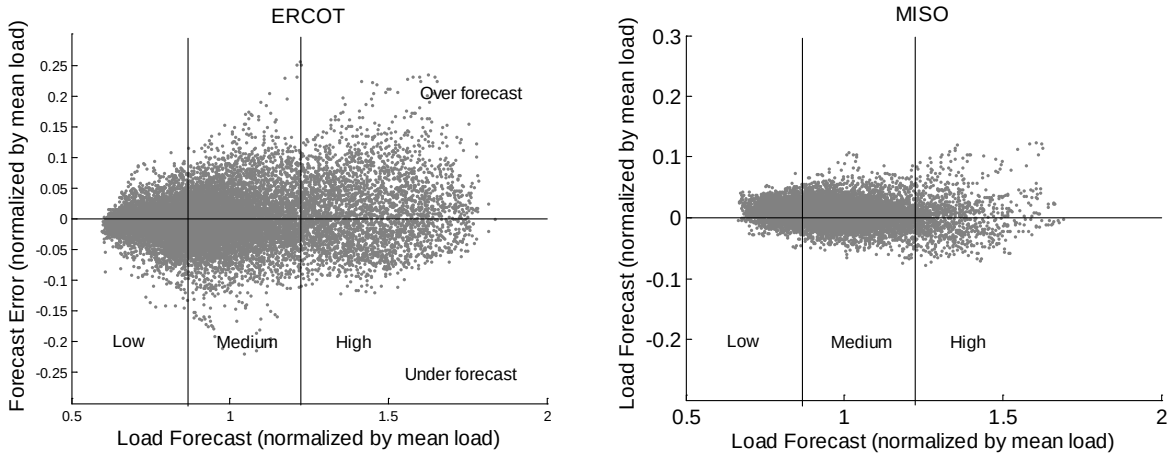

Figure 3: Day-ahead load forecast errors plotted against the load forecast values for ERCOT and MISO. The vertical lines are at 90 and 120% of the mean load.

We used the @Risk software package to fit parametric distributions to load forecast errors in ERCOT and MISO. Even though no distributions passed a Pearson's chi-squared test, the logistic distribution provided the best fit among the distributions tested, in both sets of load forecast errors, as measured by likelihood values (figure 4). In agreement with Hodge et al. (2012), we found that the actual load forecast error distribution has more mass around zero than a normal probability density function (PDF) would predict.

Figure 4 shows histograms of the load forecast errors normalized by mean load forecast with fitted logistic distributions for ERCOT and MISO. A separate logistic distribution was fit to each load forecast bin.

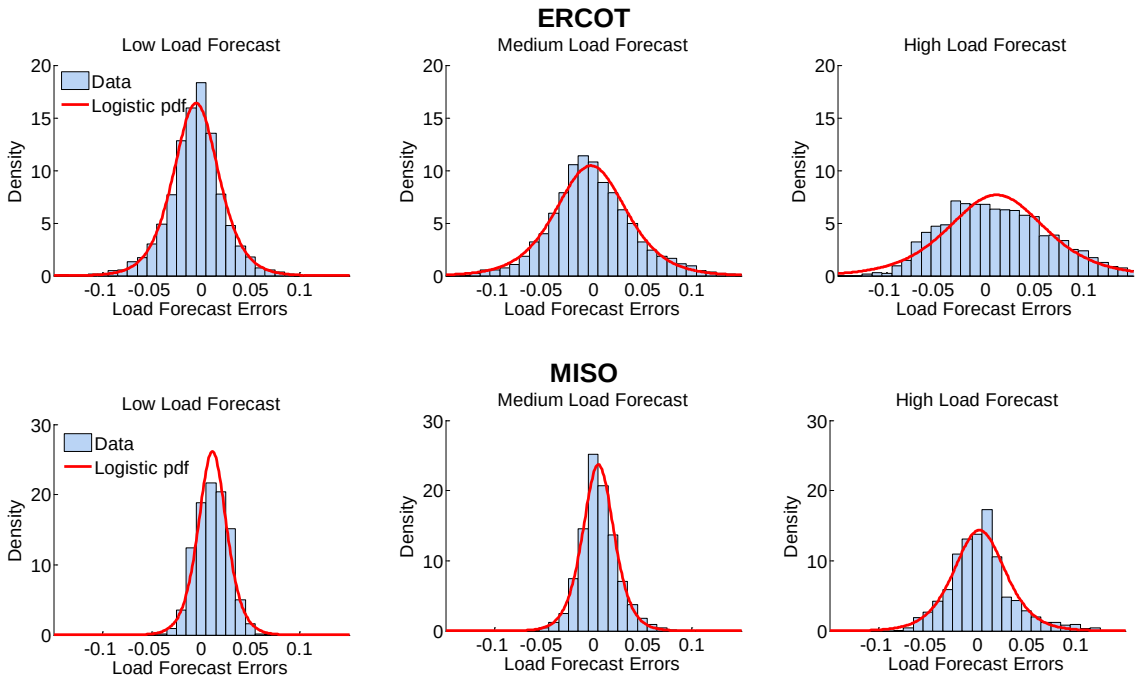

Figure 4: Load forecast errors for ERCOT (top) and MISO (bottom) with data separated into three different load forecast classes. All values are normalized by the mean load forecast. Low forecasts include all forecasts less than 90% of the mean forecast; medium forecasts are between 90 and 120% of the mean forecast; and high forecasts are greater than 120% of the mean forecast. Histogram bars show the relative frequency of the actual data while solid lines show the fitted logistic distributions.

3.2 Day-ahead wind forecast uncertainty

In comparison to day-ahead load forecasts, day-ahead wind forecasts have much greater relative uncertainty. Wind forecast error distributions also differ from load forecast error distributions in that they become highly skewed for low and high wind forecasts. The plots in figure 5 show hourly wind forecast errors plotted against wind forecast values in ERCOT and MISO. All values are shown as a fraction of installed wind capacity. At low wind power forecasts, the errors tend to be more negative while high wind power forecasts produce more positive forecasts.

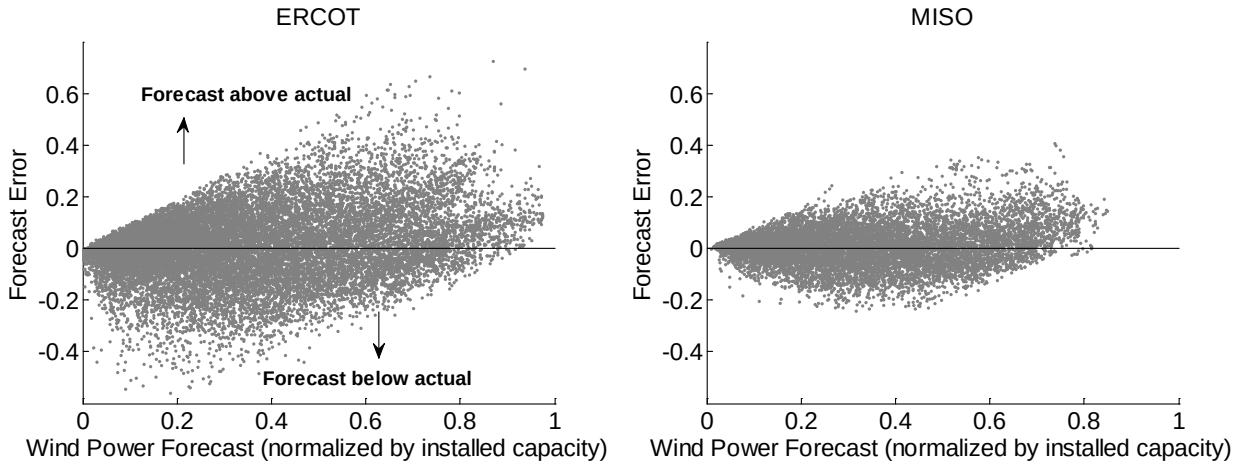

Figure 5: Day-ahead wind forecast errors (vertical axis) plotted against the day-ahead wind forecast values (horizontal axis) in ERCOT and MISO. All values are expressed as a ratio of installed wind capacity.

In order to account for the dependence of wind forecast error distributions on the wind forecast level, we used the logit-normal model to represent wind forecast errors as described in Mauch et al. (2012) and briefly in the online supplementary data. This model is illustrated in figure 6 for ERCOT and MISO wind forecast data. Error distributions are negatively skewed at the low forecasts and positively skewed at the high forecasts. The fit at low and medium forecasts is much better due to the lack of samples at the high end of the forecast range.

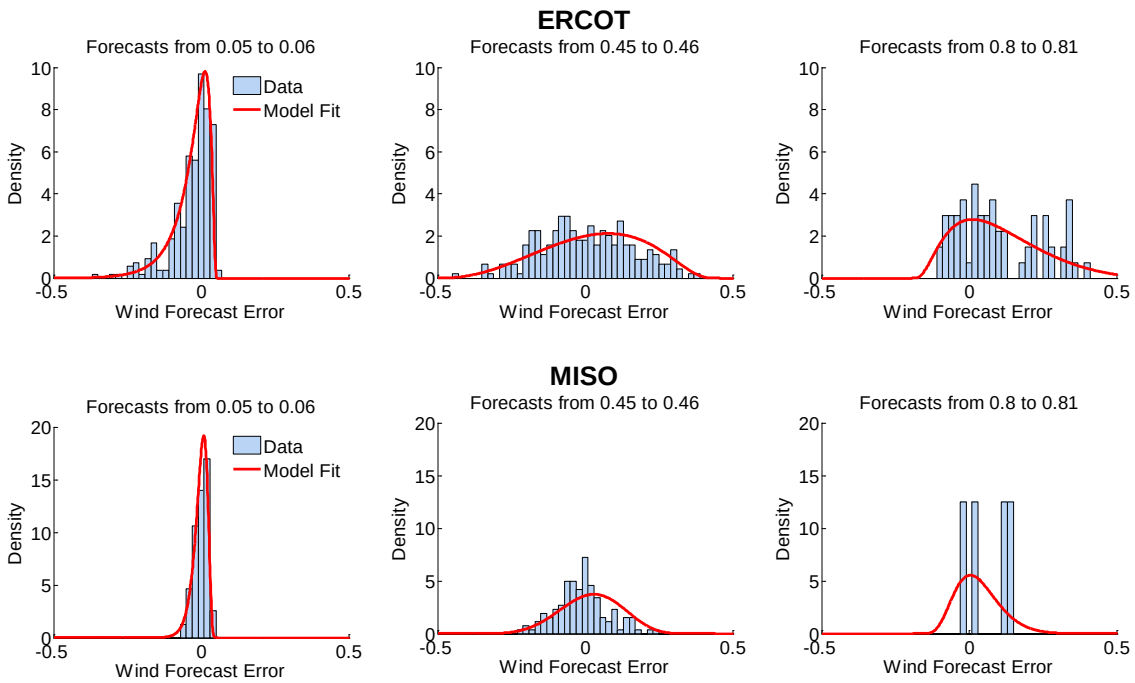

Figure 6: Wind power forecast error distributions in ERCOT (top) and MISO (bottom) at three different wind forecasts. All values are normalized by the installed wind capacity. Histogram bars show the relative frequency of the actual data while solid lines show the fitted distribution resulting from the logit-normal model.

3.3 Day-ahead net load uncertainty

Net load is defined as load (L) minus wind (W) power

$$N = L - W\,. \tag{1}$$

The actual (subscript A) levels of load and wind subtracted from the forecasted values (subscript F) give the net load forecast errors

$$err_N = \left(L_F - W_F\right) - \left(L_A - W_A\right). \tag{2}$$

Rearranging terms gives

$$err_N = \left(L_F - L_A\right) - \left(W_F - W_A\right), \tag{3}$$

$$err_N = err_L - err_W\,. \tag{4}$$

Load forecast errors and wind forecast errors are commonly assumed to be independent variables (Matos and Bessa, 2009; Ortega-Vazquez and Kirschen, 2009). The correlation coefficients of wind and load forecast errors in our data were 0.09 for ERCOT and 0.05 for MISO (both significant at the 95%

level). We assume uncorrelated wind and load forecast errors here. However, the empirical data show that the correlation coefficient of wind and load forecast errors varied over a wide range and we discuss the implications of correlation between wind and load forecast errors in the online supplementary data. With uncorrelated variables, the PDF of the net load errors is derived by taking the cross-correlation of the load errors and the negative of the wind errors. The integral was evaluated by numerical integration using Simpson quadrature.

$$f_{err_N}(err_N) = \int_{-\infty}^{\infty} f_{err_L}(x) f_{err_W}(err_N - x)dx \quad (5)$$

The cumulative distribution function (CDF) is then the integral of the PDF, which allows one to determine confidence intervals for a desired reliability level.

$$F_{err_N}(err_N) = \int_{-\infty}^{err_N} f_{err_N}(z)dz \quad (6)$$

Figure 7 shows CDFs for the load and net load errors calculated using data from ERCOT for a medium load forecast (90% to 120% of the mean load) and wind forecast level of 5,000 MW with 10,000 MW of installed wind capacity. Ninety-five percent of the net load errors range from -4,650 MW to 3,850 MW. In order to cover this level of uncertainty, a grid must have 4,650 MW of excess dispatchable generation capacity available to cover under forecasts and 3,850 MW of down generation capacity to cover over forecasts. Our analysis focuses on under forecast errors, which require additional generation capacity to be brought online quickly.

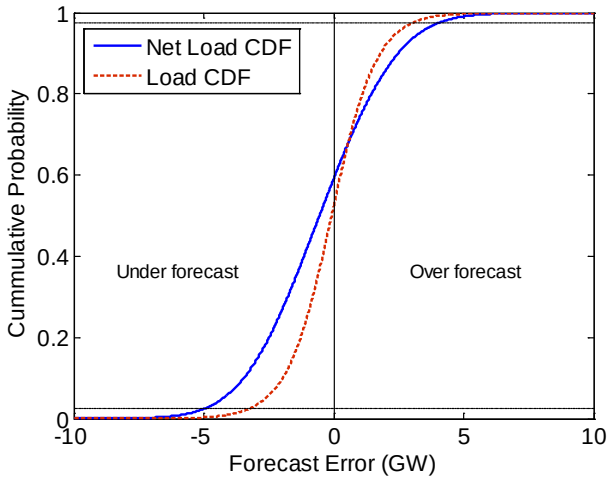

Figure 7: Cumulative distribution functions of net load errors (solid line) and load errors (dashed line) produced with the statistical model of net load uncertainty fit to data from ERCOT. The two dashed horizontal lines represent the 2.5th and 97.5th percentiles spanning 95% of the forecast errors.

Considering only the errors that result from an under forecast of net load, we compute the probability of the forecast error being less than some given value conditioned on the event that the forecast error is negative.

$$P\left(err_N \le z \mid err_N \le 0\right) = \frac{F_{err_N}\left(err_N\right)}{F_{err_N}\left(err_N = 0\right)} \tag{7}$$

Using (7), we calculate the value for *z* that gives a probability of 0.05 to get the generation capacity required to cover 95% of potential under forecast errors.

4. Results

During the interval our data were collected, ERCOT's installed wind capacity increased from 8.3 GW to 9.5 GW, and MISO's wind capacity increased from 9.1 GW to 10.8 GW. We scaled the wind data to simulate an installed wind capacity of 10 GW in both grids and compared dispatchable generation capacity requirements due to wind uncertainty for both grids.

We assume a system operator procures reserves in the form of dispatchable capacity during day-ahead operation planning. The amount of reserves procured at this stage will be augmented with energy traded on the spot market during the dispatch day. We use the ERCOT target of covering 95% of day-

ahead forecast errors with operational reserves in our analysis. It should be noted that reserves to balance wind forecast errors can be procured in multiple time horizons other than day-ahead. There is a trade-off between procuring reserves closer to the dispatch interval and ensuring day-ahead reliability that we do not explore in this paper.

We applied the analysis described in the previous section to wind and load forecast data from ERCOT and MISO to plot the dispatchable generation capacity required for 95% of the net load under forecast errors. Figure 8 displays the required levels of dispatchable capacity as a function of the day-ahead wind power forecast for one period during which the load forecast is near the mean value (medium load). The low and high load forecast bins are shown in later graphs. The 95th percentile of load under-forecast errors in ERCOT is 3,100 MW and 2,200 MW in MISO. Wind forecast uncertainty in ERCOT increases the required capacity to 5,300 MW at a wind power forecast of 7,500 MW. In MISO the total capacity required to cover 95% of net load errors is 3,100 MW at a wind forecast of 6,000 MW. The greater accuracy in MISO wind and load forecasts leads to less net load uncertainty compared to ERCOT (table 1).

Wind uncertainty increases the additional dispatchable capacity requirement in ERCOT up to 2,200 MW which is equal to the maximum capacity required for net load forecast errors (5,300 MW at a wind forecast of 7,500 MW) minus the capacity needed to cover load forecast errors (3,100 MW). In MISO (with its lower wind forecast uncertainty), the range is zero to 900 MW, with the latter occurring at a wind forecast of 6,000 MW.

The median wind forecasts during the observation periods were 3,100 MW in ERCOT and 3,200 MW in MISO so half the time wind uncertainty contributes less than a few hundred MW of dispatchable capacity requirement. The high end of the operating reserve requirement does not indicate the additional reserves due to wind; it indicates the reserve requirement at maximum wind uncertainty.

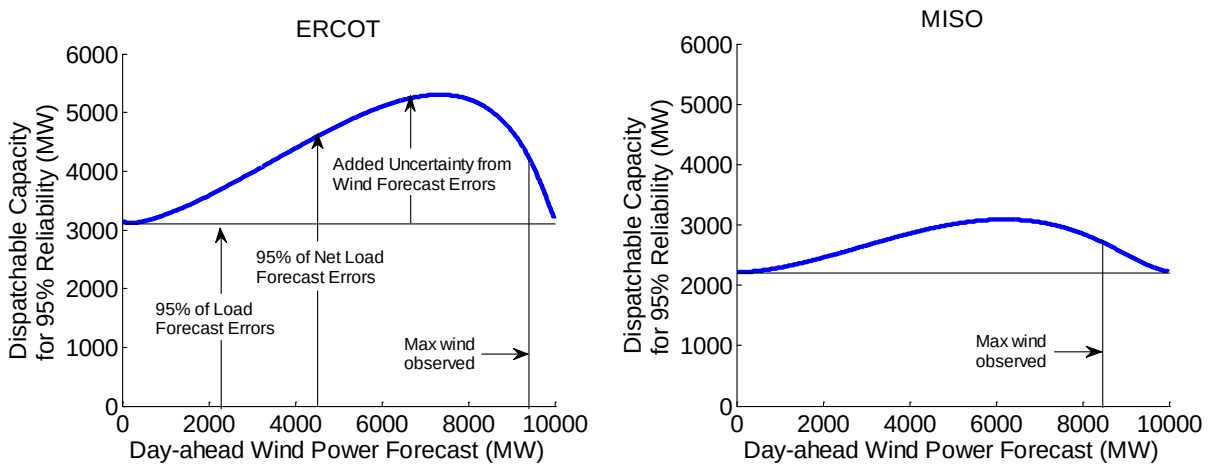

Figure 8: Dispatchable generation capacity required to cover 95% of day-ahead net load under forecast errors in ERCOT and MISO when load forecasts are in the range 90% to 120% of mean load forecast. Each graph shows the 95th percentile of load forecast errors as a horizontal line. Net load forecast uncertainty converges to load forecast uncertainty at zero wind forecast and also at the maximum wind forecast.

We chose the ERCOT day-ahead reliability level of 95%, but some system operators may choose other day-ahead reliability levels, depending on operational policies. Using medium load forecast levels, figure 9 shows the dispatchable generation capacity required to provide day-ahead reliability levels from 95% to 99% as a function of the day-ahead wind forecast. Providing an increase in day-ahead reliability from 95% to 99% in ERCOT requires 1,500 MW more dispatchable capacity. In MISO, 1,000 MW of additional capacity is required.

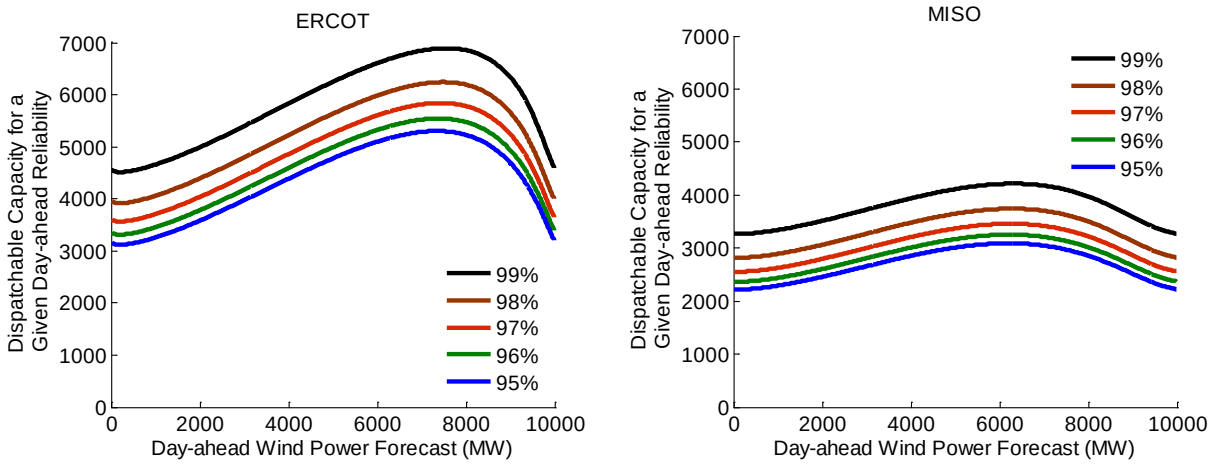

Figure 9: Dispatchable generation capacity required to cover 95% to 99% of net load forecast errors in ERCOT and MISO for load forecasts in the range 90% and 120% of mean load forecast.

Figure 10 shows the effect of the forecasted load on the net load uncertainty. At high load forecasts the uncertainty associated with the load forecast increases, and so does the net load forecast uncertainty. Each plot below displays separate curves for three load forecast levels defined in subsection 3.1. In ERCOT, the three curves are evenly spaced as load uncertainty increased gradually with the load forecast value. The MISO load uncertainty increased more abruptly at high load forecasts.

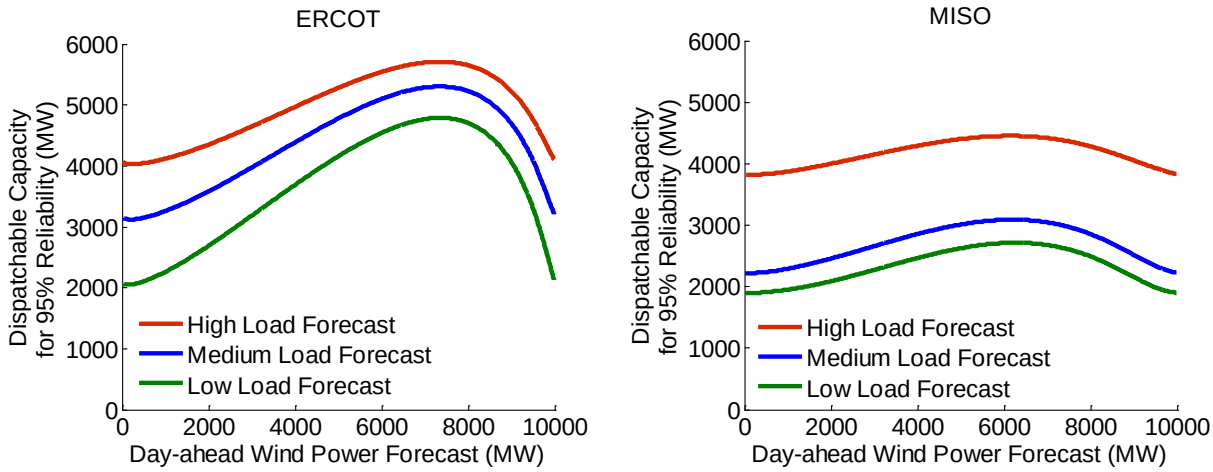

Figure 10: Amount of dispatchable generation capacity required to cover 95% of net load under forecast errors as a function of wind forecast level for 10 GW of installed wind capacity for three different load forecast levels. Back-up requirements peak in ERCOT at a wind forecast of 7,500 MW and in MISO at 6,000 MW.

The graphs in figure 10 show that the 95th percentile of net load under forecasts in ERCOT ranges from 2,100 (low load forecast with no wind) to 5,700 MW (high load forecast with 7,500 MW wind forecast). In MISO the range is from 1,900 MW to 4,500 MW depending on the load and wind forecasts for 10 GW of wind capacity. The online supplemental material contains more discussion on the difference of net load forecast uncertainty between ERCOT and MISO.

We now consider the operating reserves that will be required to balance additional forecast uncertainty for future levels of installed wind capacity. The distribution of wind forecast errors is the metric of interest for reserve allocation, rather than the mean or root mean square forecast error. We observe from figure 4 that the distribution of wind forecast errors is much narrower for MISO than for

ERCOT. Both grids have very close to the same amount of wind. Thus we conclude that the geographic dispersion component accounts for much of the difference in forecast error.

Similarly, Focken et al. (2002) showed that the standard deviation of wind forecast errors decreases as a function of the area covered by the wind farms. They found that the installed wind capacity was less important than the area covered. In their results, the 36-hour look-ahead forecast error standard deviation decreased roughly 28% when the area doubled (their figure 9). While Focken et al.'s work was based on German data, Katzenstein et al. (2010) found similar results with ERCOT data when analyzing wind output standard deviation.

However, it can also be argued that holding the geographic area constant while increasing the number of wind turbines will decrease the forecast error and narrow the error distribution. While we do not observe this comparing MISO to ERCOT, we account for both possibilities in what follows. As a worst-case scenario, we assume wind is added to the grid in a manner that the wind forecast accuracy stays constant. This assumes future wind farms cluster in the same areas as existing wind farms. As a best-case scenario, we consider adding more wind away from the existing wind farms to spread the wind over a wider area. In this scenario we reduced the wind forecast errors to represent improved forecasts, as described below. Note that in both scenarios the wind forecast error distribution shape is assumed to be the same, only the width changes.

In order to simulate improved forecasts, we used the results of Focken et al. for the wind forecast error standard deviation. In the best-case scenario, we assume the geographical area covered by wind farms doubles as installed capacity increases from 10 to 30 GW. The standard deviation of the wind forecast errors decreases by 28% over this range of installed wind capacity. This suggests that the standard deviation of wind forecast errors can be modeled as a function of installed wind capacity as

$$\sigma_W = \beta C^{\alpha} \tag{8}$$

where C is the installed capacity and α and β are constants. The values of the constants are determined with two pairs of values for σ and C. The first pair is the observed standard deviation of the forecast

errors and the installed capacity when the data were collected. The second pair is the observed standard deviation reduced by 28% and the observed installed capacity increased by a factor of three. The resulting functions are shown in figure 11. □

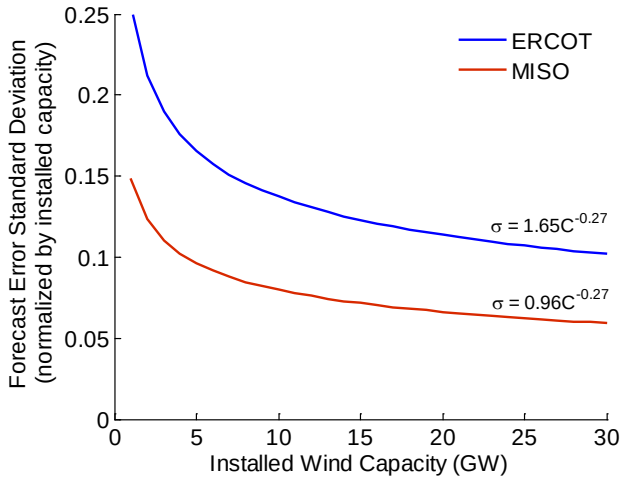

Figure 11: Standard deviation of modeled wind forecast errors as a function of installed wind capacity in ERCOT and MISO.

Observed wind forecast errors were scaled by the ratio of the simulated forecast error standard deviation to the observed standard deviation (equation 9) to achieve modeled forecast errors with the desired standard deviation. The method described here can be applied accurately without regard to these conjectures about how forecast accuracy changes as more wind is added by using the observed forecast accuracy at that larger installed capacity.

$$err_{\text{mod}} = err_{obs}\left(\frac{\sigma_{\text{mod}}}{\sigma_{obs}}\right) \tag{9}$$

Whether wind forecasts will become more accurate is uncertain. MISO wind farms seem to already exhibit close to the maximum geographical dispersal. The ERCOT situation is much different. Wind is highly concentrated in the western section and future wind developments along the Gulf coast may reduce the correlation of output between wind farms (see figure 1). □

We estimated the maximum amount of dispatchable generation required to balance wind forecast errors if installed wind capacity is increased to 30 GW (approximately a three-fold increase from current

ERCOT or MISO installed wind). To be clear, this does not indicate that new capacity must be built for future wind. Rather a portion of the existing capacity will provide more reserves as wind displaces energy deployments. For a range of wind capacities up to 30 GW, we determined the maximum amount of dispatchable generation required to cover 95% of the net load forecast errors for ERCOT and MISO. For example, from figure 10 the maximum capacity required for net load errors is 5,700 MW in ERCOT and 4,500 MW in MISO when wind capacity is 10 GW. The curves in figure 12 show the maximum dispatchable generation as a function of the installed wind capacity for the worst-case scenario (wind forecast accuracy remains constant) and the best-case scenario (improved wind forecast leads to forecast errors scaled down). We modeled the worst-case scenario by linearly scaling up the wind forecast data to simulate greater levels of wind capacity. In the best-case scenario with improved forecasts, the wind forecast errors were scaled such that the standard deviation of the normalized forecast errors decreased with higher installed capacity according to figure 11. In ERCOT, day-ahead reserves required with 30 GW of installed capacity range from 8,700 MW to 13,000 MW (4,600 MW to 8,900 MW due to wind). Thus, roughly 16% to 30% of this capacity would be needed in the form of dispatchable generation to cover wind forecast uncertainty. Load data is held constant. In MISO the values range from 6,000 MW to 7,800 MW (2,100 MW to 3,900 MW due to wind). Approximately 7% to 13% of MISO wind capacity is required in the form of dispatchable generation to cover wind forecast uncertainty. Once again, this does not indicate that new capacity must be built for future wind. Rather a portion of the existing capacity will provide more reserves as wind displaces energy deployments.

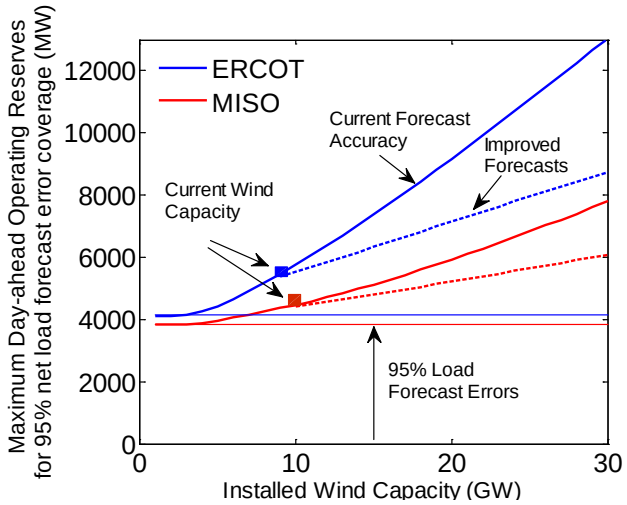

Figure 12: Dispatchable generation capacity requirements for maximum wind forecast uncertainty for installed wind capacity up to 30 GW in ERCOT and MISO. Horizontal lines show the level of capacity required to cover load forecast errors at high load forecasts. Solid lines show operating reserves required for 95% of net load errors with current wind forecast accuracy. Dashed lines show the results with improved wind forecasts as defined above for wind capacity above 10 GW. Maximum wind forecast uncertainty is assumed to occur for wind forecasts of 75% of installed capacity in ERCOT and 60% of installed capacity in MISO. Current wind capacity refers to the time in which the data were collected.

Assuming constant wind capacity factors in ERCOT (CF=0.35) and MISO (CF=0.33), we calculate day-ahead reserves needed for wind capacity as a function of the proportion of energy produced by wind. In figure 13, the additional dispatchable capacity represents the maximum day-ahead reserves required beyond that which is needed to cover load forecast errors with a high load forecast. For example, in ERCOT with 10 GW of wind capacity nearly 10% of the load is served by wind. At this capacity the maximum value of the 95th percentile for net load is 5,700 MW and the 95th percentile for load forecast errors is 4100 MW meaning the wind adds an additional 1600 MW of reserve capacity to cover 95% of day-ahead forecast errors. In MISO, 10 GW of wind serves 5.5% of load and requires an additional 600 MW of reserves beyond that which is needed for load forecast uncertainty. In order to get 30% of the total generation from wind, ERCOT would require just over 30 GW of installed wind capacity while MISO would need 54 GW of installed wind capacity at current load levels. While MISO has tighter wind forecasts, it has a much larger load. These two factors nearly cancel each other making the additional capacity requirement on a MW basis equal for both grids when compared on a wind percentage basis.

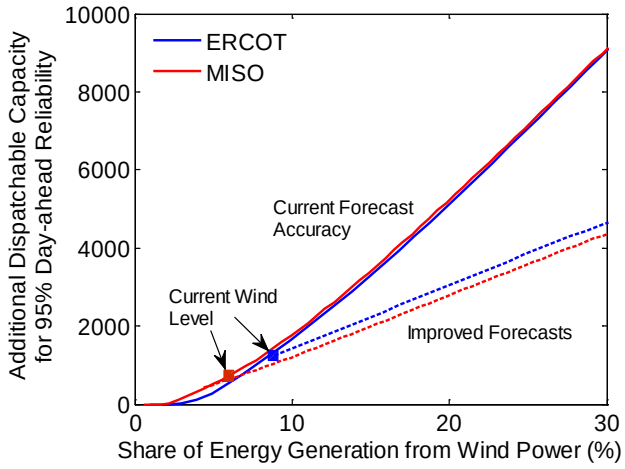

Figure 13: Additional day-ahead reserve capacity for maximum wind forecast uncertainty for a range of wind penetration values in ERCOT and MISO. In this figure the horizontal axis is the percentage of load served by wind power. Solid lines assume no change in wind forecast accuracy. Dashed lines show the effect of improved forecasts. Maximum wind forecast uncertainty is assumed to occur for wind forecasts of 75% of installed capacity in ERCOT and 60% of installed capacity in MISO. Current wind level refers to the time in which the data were collected.

Figure 14 presents the additional day-ahead reserves required to compensate for net load forecast errors as a percentage of peak load, again as a function of the penetration of wind power. This figure may provide useful bounds on the reserves that will be required as wind's share of generation increases.

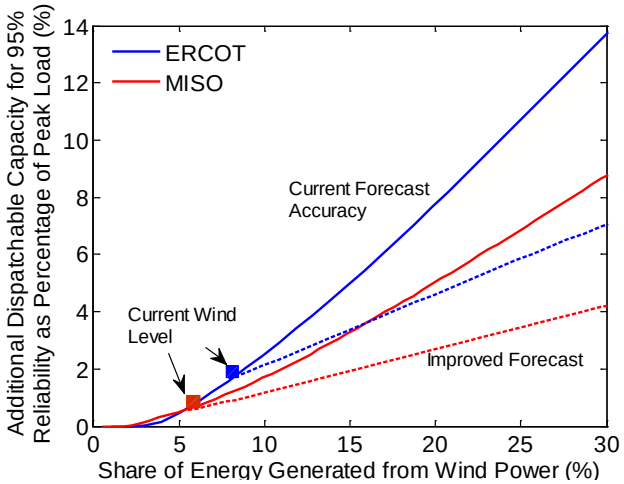

Figure 14: Additional day-ahead reserve capacity for maximum wind forecast uncertainty as a percentage of peak load for a range of wind penetration values in ERCOT and MISO. Maximum wind forecast uncertainty is assumed to occur for wind forecasts of 75% of installed capacity in ERCOT and 60% of installed capacity in MISO. Current wind level refers to the time in which the data were collected.

We now compare the results of our model with the analysis performed in ERCOT to determine operational reserves as defined in ERCOT (2012). ERCOT procures day-ahead operating reserves based upon an analysis of forecast uncertainty from forecasts submitted at midnight of the operating day. Operating reserves are procured such that the sum of regulation up, non-spinning reserves and 500 MW of responsive reserves cover the 95th percentile of negative net load forecast errors. Here, we are concerned with day-ahead uncertainty and, as such, we analyze uncertainty using forecasts submitted at approximately 6:00 am before the operating day.

Additionally, our analysis differs from ERCOT's method in that we assume dynamic procurements each hour based on forecast values whereas ERCOT sets monthly reserve requirements based on an analysis of forecast data for the previous month and the same month of the previous year. Our model estimates the range of reserves based on the 95th percentile of day-ahead wind and load forecast errors would be from 2,100 MW to 5,700 MW. Most hours would be at the low end of the range given the ~35% capacity factor of wind in ERCOT.

Maggio (2012) showed that monthly averages for the combination of regulation up and non-spinning procurements ranged from 2,100 MW to 2,500 MW during an eleven-month period in 2011 when approximately 9,500 MW of installed wind capacity existed in ERCOT. Adding the 500 MW of responsive reserves, the total of ERCOT's procurement was on average 2,600 MW to 3,000 MW to cover the 95th percentile of net load uncertainty. Maggio's analysis also estimated that between 110 MW and 800 MW of the reserve procurement was attributable to wind forecast uncertainty (monthly averages). These are monthly averages and are influenced by the system wide capacity factor in ERCOT. We estimate that in certain hours wind uncertainty can be much more significant (over 2000 MW). However, as stated above, half of the wind forecast values are less than 3100 MW, which adds less than 1000 MW to the reserve requirements depending on the load forecast level, in good agreement with the reserves ERCOT currently procures.

5. Conclusion

Proper quantification of wind forecast uncertainty and how it affects net load uncertainty is essential for optimal reserve procurements. Currently, most U.S. grids do not have high enough levels of wind power to make this a major concern, but this situation is likely to change. We used an empirical analysis of wind forecast uncertainty and load forecast uncertainty to develop a method that can be used in making day-ahead procurement decisions.

We present a method based on observed wind and load forecast distributions. Using data from ERCOT and MISO, we calculated the amount of dispatchable generation capacity required to cover the day-ahead wind and load forecast errors at different desired confidence levels. In order to cover 95% of the day-ahead net load under-forecast errors, reserve levels ranged from 2,100 to 5,700 MW in ERCOT and 1,900 to 4,500 MW for MISO, depending on the load and wind forecasts. Hence, decisions on generation capacity procurement to cover the day-ahead forecast uncertainty must consider the systematic nature of wind and load forecast uncertainty. As wind power uncertainty begins to dominate load uncertainty, system operators will have to adjust decision-making to account for the wind uncertainty.

We also simulated future grids with higher levels of wind capacity and estimated that in ERCOT each additional MW of installed wind capacity would require 0.16 to 0.30 MW of dispatchable capacity to correct day-ahead forecast errors depending on the accuracy of the forecasts (see figure 12). In MISO this range is 0.07 and 0.13 MW.

Our analysis focused solely on the day-ahead uncertainty. However, ERCOT uses a shorter time horizon to determine reserve requirements. As the decision time approaches, more information becomes known and uncertainty is reduced. We chose to analyze day-ahead forecast data because many operating decisions are made in that time frame. However, procuring reserves in a shorter time frame (say 12 or 6 hours in advance) would allow reduced reserve requirements. There is a trade-off between look-ahead time and the number of procurement periods a system operator should consider.

Ramp rate requirements are a factor when planning for hourly changes in net load uncertainty. We did not incorporate this aspect of reserve planning, but it is an important issue that requires further

investigation. Nor did we consider the economics of ensuring enough dispatchable generation for wind power uncertainty, since this is highly dependent on factors outside the scope of this research. However, we noted that the non-spinning reserves used by ERCOT to balance wind forecast errors are relatively low cost compared to other, faster types of reserves. Recent studies have estimated the operational integration costs of wind power from $2.5 to $7 per MWh of wind energy generation which includes balancing variability and forecast uncertainty. Finally, our work did not take into account grid contingencies leading to forced generator outages. This risk is generally required to be covered with reserves equal to the amount of generation loss from the largest potential contingency in the grid.

This work shows that ensuring a particular level of reliability in an electric system with significant levels of wind power capacity requires hourly levels of reserve capacity that depend on the hourly predictions for load and wind power. We quantify these reserve level requirements as a function of the load and wind power prediction.

Wind power is likely to play a larger role in electricity production in future grids. We show that in ERCOT, as installed wind capacity reaches 30 GW, up to 30% of this capacity will need to be matched with dispatchable capacity to cover wind forecast uncertainty. In MISO, up to 13% of the installed wind capacity must be matched with dispatchable capacity. We note, however, that the numeric values are not transferable to other systems but the method presented in this paper can be applied to do system-specific analysis.

Acknowledgements

This work was supported in part by the Doris Duke Charitable Foundation, the R.K. Mellon Foundation and the Heinz Endowments for support of the RenewElec program at Carnegie Mellon University. This research was also supported in part by the Climate and Energy Decision Making (CEDM) center created through a cooperative agreement between the National Science Foundation (SES-0949710) and Carnegie Mellon University. Brandon Mauch was supported by a fellowship from the Portuguese Foundation for Science and Technology (Fundação para a Ciência e a Tecnologia), number SFRH/BD/33764/2009. The

authors would like to thank Dr. Mark Handschy for his helpful comments. They are also grateful for the data provided by AWS Truepower.

References

1. American Wind Energy Association (AWEA), website, last accessed February 2013 http://www.awea.org/learnabout/industry_stats/index.cfm
2. Bludszuweit, H., Dominguez-Navarro, J.A., Llombart, A., 2008. Statistical analysis of wind power forecast error, IEEE Transactions on Power Systems, 23 (3), pp. 983-991
3. Botterud, A., Wang, J., Miranda, V., Bessa, R.J., (2010). Wind power forecasting in U.S. electricity markets, The Electricity Journal, Vol. 23, 3, 71–82
4. Bouffard, F., Galiana, F.D., 2008. Stochastic security for operations planning with significant wind power generation, 2008 IEEE Power and Energy Society General Meeting - Conversion and Delivery of Electrical Energy in the 21st Century, pp. 1-11
5. Doherty, R., O'Malley, M., 2005. A new approach to quantify reserve demand in systems with significant installed wind capacity, IEEE Transactions on Power Systems, 20 (2), pp. 587- 595
6. EIA, 2013. Electric Power Monthly January 2013, Energy Information Administration, DOE/EIA-0226 (2012/01(11)), http://www.eia.gov/beta/epm/pdf/epm.pdf
7. Elektrotek, 2003. We Energies energy system operations impacts of wind generation integration study, Electrotek Concepts, Inc., http://www.uwig.org/weenergieswindimpacts_finalreport.pdf
8. Enernex, 2007. Final report – 2006 Avista Corporation wind intergration study, Enernex Corporation, http://www.uwig.org/avistawindintegrationstudy.pdf
9. ERCOT, (2012). ERCOT Methodologies for Determining Ancillary Service Requirements, April, 2012
10. Fertig, E., Apt, J., Jaramillo, P., Katzenstein, W., 2012. The effect of long-distance interconnection on wind power variability, Environmental Research Letters, 7 (3),
11. Focken, U., Lange, M., Mönnich, K., Waldl, H.P., Beyer, H.G., Luig, A., 2002. Short-term prediction of the aggregated power output of wind farms—a statistical analysis of the reduction of the prediction error by spatial smoothing effects, Journal of Wind Engineering and Industrial Aerodynamics, 90, pp. 231–246
12. Hodge, B., Florita, A., Orwig, K., Lew, D., Milligan, M., 2012. A comparison of wind power and load forecasting distributions, 2012 World Renewable Energy Forum, NREL/CP-5500-54384, http://www.nrel.gov/docs/fy12osti/54384.pdf
13. Holttinen, H., Milligan, M., Kirby, B., Acker, T., Neimane, T., Molinski, T., 2008. Using standard deviation as a measure of increased operational reserve requirement for wind power, Wind Engineering, 32 (4), pp. 355-378
14. Katzenstein, W., Fertig, E., Apt, J., 2010. The variability of interconnected wind plants, Energy Policy, 38 (8), pp. 4400–4410
15. Kehler, J., Ming, H., McMullen, M., Blatchford, J., 2010. ISO perspective and experience with integrating wind power forecasts into operations, 2010 IEEE Power and Energy Society General Meeting, pp. 1-5

16. Lange, M., On the uncertainty of wind power predictions—Analysis of the forecast accuracy and statistical distribution of errors, Journal of Solar Energy Engineering, Vol. 127, (2005) 177–184
17. Lowery, C., O'Malley, M., 2012. Impact of wind forecast error statistics upon unit commitment, Sustainable Energy, IEEE Transactions on, 3 (4), pp.760-768.
18. Maggio, D.J. 2012. Impacts of wind-powered generation resource integration on prices in the ERCOT nodal market. In 2012 IEEE Power and Energy Society General Meeting, pp.1-4
19. Makarov, Y.V., Etingov, P.V., Jian M., Zhenyu H., Subbarao, K., 2011. Incorporating uncertainty of wind power generation forecast into power system operation, dispatch, and unit commitment procedures, Sustainable Energy, IEEE Transactions on, 2 (4), pp.433-442
20. Matos, M.A., Bessa, R., 2009. Operating reserve adequacy evaluation using uncertainties of wind power forecast, PowerTech, 2009 IEEE Bucharest, pp.1-8
21. Mauch, B., Carvalho, P., Apt, J., Small, M., 2012. An effective method for modeling wind power forecast uncertainty, Energy Systems, DOI 10.1007/s12667-013-0083-3, 2013
22. MISO Reliability Subcommittee Report June 27, 2012. https://www.misoenergy.org/Library/Repository/Meeting Material/Stakeholder/RSC/2012/20120626/20120626 RSC Item 08 Wind Curtailment Data.pdf
23. Ortega-Vazquez, M.A., Kirschen, D.S., 2009. Estimating the spinning reserve requirements in systems with significant wind power generation penetration, IEEE Transactions on Power Systems, 24 (1), pp. 114-124
24. Rogers, J., Fink, S., Porter, K., 2010. Examples of wind energy curtailment practices, NREL Subcontract Report, NREL/SR-550-48737
25. U.S. Department of Energy, Strategies and decision support systems for integrating variable energy resources, Technical Report, 2011, online: http://www1.eere.energy.gov/wind/pdfs/doe_wind_integration_report.pdf
26. Wang, J., Shahidehpour, M., Li, Z., 2008. Security-constrained unit commitment with volatile wind power generation, Power Systems, IEEE Transactions on, 23 (3), pp. 1319-1327
27. Wilkes, J., Moccia, J., Drangan, M., 2012. Wind in power: 2011 European wind statistics, European Wind Energy Association Technical Report, http://www.ewea.org/ fileadmin/ewea_documents/documents/publications/statistics/Stats_2011.pdf
28. Xie, L., Carvalho, P.M.S., Ferreira, L.A.F.M., Juhua L., Krogh, B.H., Popli, N., Ilić, M.D., 2011. Wind integration in power systems: operational challenges and possible solutions, Proceedings of the IEEE, 99 (1), pp.214-232

Online supplementary data

1. Wind forecast error logit-normal model

Using this method, we fit normal distributions to logit transformations of hourly, day-ahead wind forecasts (F) and observed wind power (W) values. Both variables are normalized by the installed wind capacity in order to ensure that F and W have ranges from 0 to 1. The resulting transformed variables range from negative to positive infinity

$$F^* = \ln\left(\frac{F}{1-F}\right) \qquad W^* = \ln\left(\frac{W}{1-W}\right). \tag{10}$$

Once the transformed variables are fit to a normal distribution, confidence intervals are straightforward to calculate and transform back into the original variable space. Different confidence levels are displayed as a function of the wind forecast level in figure 15 using logit-normal parameters derived from fitting the data from figure 5 in the main text.

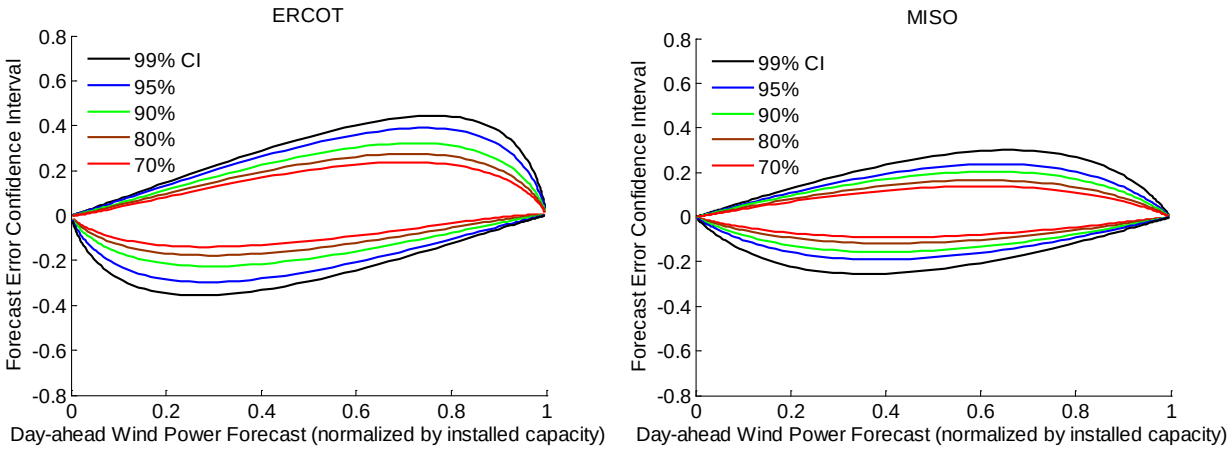

Figure 15: Confidence levels for the data in figure 5 calculated with the logit-normal model.

If the logit transformation of a variable is normally distributed, $N(\mu, \sigma^2)$, then the variable itself is distributed logit-normal, $LN(\mu, \sigma^2)$. In this model the wind forecast values and observed wind values are assumed to be jointly distributed logit-normal with the joint probability density function

$$f_{F,W}(F,W)=\left(\frac{1}{2\pi\sigma_F\sigma_W\sqrt{1-\rho^2}F(1-F)(1-W)}\right)e^{\left(-\frac{1}{2(1-\rho^2)}\left[\frac{(F^*-\mu_F)^2}{\sigma_F^2}+\frac{(W^*-\mu_W)^2}{\sigma_W^2}-\frac{2\rho(F^*-\mu_F)(W^*-\mu_W)}{\sigma_F\sigma_W}\right]\right)}. \quad (11)$$

The conditional distribution of observed wind power given a wind forecast level ($W|F$) then becomes

$$f_{W|F}(W\mid F)=\left(\frac{1}{\sqrt{2\pi}\sigma_{W|F}W(1-W)}\right)e^{\left(-\frac{(W^*-\mu_{W|F})^2}{2\sigma_{W|F}^2}\right)}. \quad (12)$$

Wind forecast errors are defined as the forecast level minus the observed wind value. Forecast error distributions are simply the forecast value minus the expression in (11).

$$f_{err|F}(err\mid F)=F-\left(\frac{1}{\sqrt{2\pi}\sigma_{W|F}W(1-W)}\right)e^{\left(-\frac{(W^*-\mu_{W|F})^2}{2\sigma_{W|F}^2}\right)}. \quad (13)$$

2. Net Load Uncertainty in ERCOT and MISO

As discussed in the results of the main section, reserve capacity increases due to wind forecast uncertainty can be as high as 2,200 MW in ERCOT and 900 MW in MISO with medium load forecasts. The large difference in the additional generation requirements is due to the size of the forecast confidence intervals and the ratio of wind-to-load uncertainty in each region (the 95th percentile positive wind error / 95th percentile negative load error). Figure 16 shows the ERCOT wind-to-load uncertainty ratios range from 1 to 2, while in MISO it is between 0.6 and 1.2. In ERCOT, during our study period, wind power would have provided 8.7 percent of the total electricity generated without curtailments (table 1 of main text). Wind power produced only 5.5 percent of the electricity in MISO. The different ratios of electricity generated from wind power in each grid contribute to the different wind-to-load uncertainty ratios.

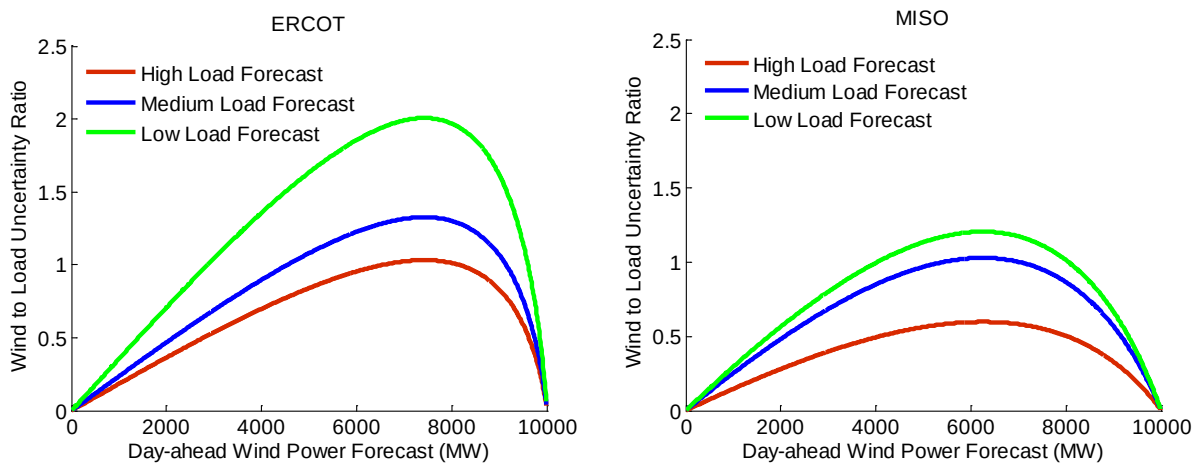

Figure 16: Ratio of the 95th percentile of positive wind forecast errors to the 95th percentile of negative load forecast errors in ERCOT and MISO with 10 GW of installed wind capacity. Wind is relatively more uncertain in ERCOT than in MISO.

Figure 17 shows the portion of reserves attributable to wind forecast uncertainty as a percentage of the wind forecast. The vertical axis is the percentage of the day-ahead wind forecast that is required to cover net load errors beyond the load errors. For example, in ERCOT a forecast for medium load and 4,000 MW of wind would require 30% of the wind forecast (1,200 MW) in addition to the capacity required to cover the day-ahead load forecast errors. In MISO, no more than 10 to 15% of the forecasted wind power must be added to day-ahead reserve levels to cover the wind uncertainty. In ERCOT the values are much higher, ranging from 25 to 40 %.

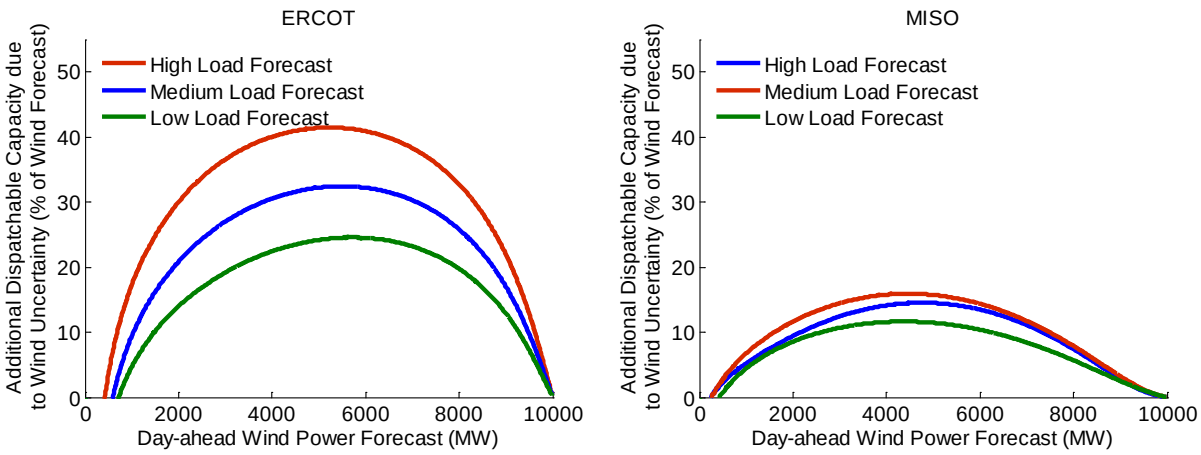

Figure 17: Additional dispatchable day-ahead generation capacity required to cover 95% of wind forecast errors shown as a percentage of the day-ahead wind forecast in ERCOT and MISO with 10 GW of installed wind capacity.

3. Correlation of wind and load forecast errors

Wind and load forecast errors are often assumed to be independent. However, this is rarely examined with data. In the ERCOT and MISO data, the correlation coefficients for wind and load forecast error time series were 0.09 and 0.05 respectively. We divided the data into subsets by hour of the day. All data were placed into one of twenty-four bins. In each hourly bin, the correlation coefficient of wind and load forecast errors were calculated (figure 18). In both ERCOT and MISO the errors are generally positively correlated. In ERCOT the correlation is significant for all but the last three hours, while MISO has values that are generally not statistically different than zero.

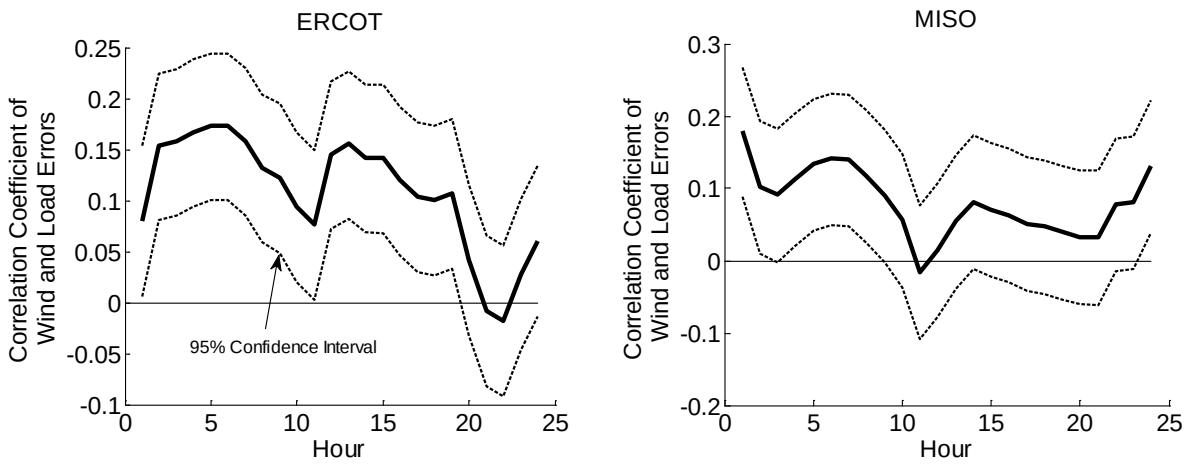

Figure 18: Correlation coefficient of wind and load forecast errors by hour of the day in ERCOT and MISO.

In ERCOT, the correlation coefficient is higher during the early morning and at midday. In MISO the coefficient is higher at midnight and in the early morning. To examine this further, we separated the data by month and by hour. Data from each month were sorted into 24 bins according to the hour. For example, we grouped all of the forecast errors that occurred in January 2009 at 10 a.m. into one bin. This produced many values for correlation coefficients. Some may be spurious due to small sample sizes. Figure 19 shows the distribution of the correlation coefficients for both ERCOT and MISO. ERCOT data covered 24 months while MISO data covered 15 month.

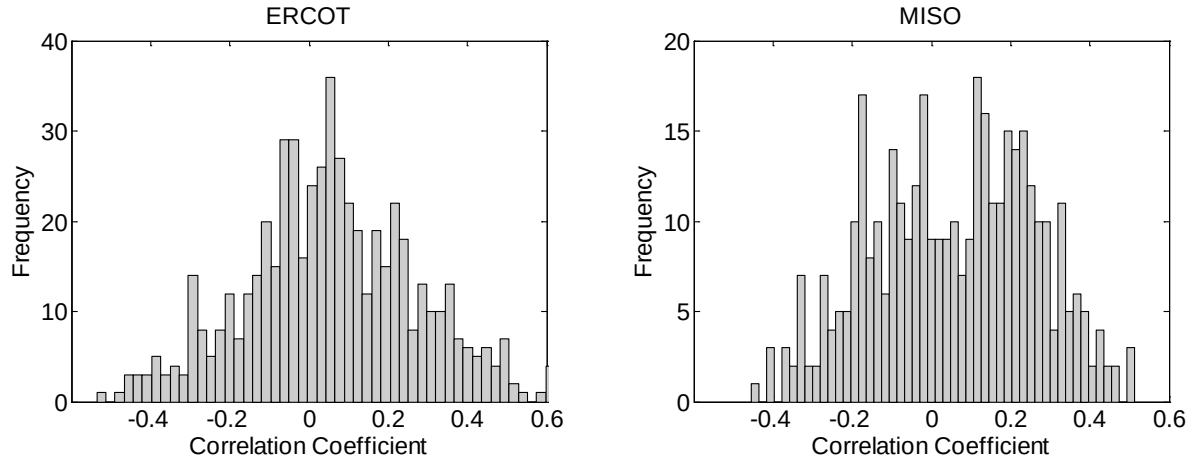

Figure 19: Frequency distribution of correlation coefficients calculated for each hour within the same month.

The data show little pattern in the correlation between wind and load errors. From the figure above, we conclude that it is possible to have significant positive and negative correlation between wind and load forecast errors.

Finally, we grouped the data according to forecast values to observe correlation when wind and load forecasts are high, medium and low. Tables 2 and 3 show the correlation coefficient calculated for 4 different levels of wind and load forecasts in ERCOT and MISO.

Table 2: Correlation coefficients calculated in ERCOT for four different forecast levels of wind and load.

ERCOT Wind and Load Forecast Correlation				
Wind Forecast as a Percentage of Installed Capacity	Load Forecast as a Percentage of Mean Load Forecast			
	LF ≤ 80%	80%≤ LF<100%	100%≤ LF<120%	LF>120%
WF ≤ 20%	0.04	0.04	0.07	0.04
20% < WF ≤ 40%	0.26	0.19	0.17	0.19
40% < WF ≤ 60%	0.26	0.09	0.05	0.12
WF > 60%	0.19	0.07	0.14	0.39

Table 3: Correlation coefficients calculated in MISO for four different forecast levels of wind and load.

MISO Wind and Load Correlation				
Wind Forecast as a Percentage of Installed Capacity	Load Forecast as a Percentage of Mean Load Forecast			
	LF ≤ 80%	80%≤ LF<100%	100%≤ LF<120%	LF>120%
WF ≤ 20%	0.17	0.03	0.05	0.07
20% < WF ≤ 40%	-0.07	0.06	0.07	0.23
40% < WF ≤ 60%	-0.02	0.14	0.07	0.26
WF > 60%	0.33	0.18	0.09	-0.01

Once again there are occasions where the errors have significant levels of correlation. The highest values occur with high levels of forecasted load and also very low levels of forecasted load. Given the tables and figures above we developed a model of the load and wind forecast errors with correlation levels ranging from -0.4 to 0.4.

We used a Monte-Carlo simulation to draw wind and load forecast errors from the same probability distributions presented in the main text. In order to create correlated errors we followed the procedure outlined below.

1. Generated correlated values (U) from a multivariate standard normal distribution.
2. Calculate the standard normal cumulative distribution values, Φ(U). These values are uniformly distributed and correlated.
3. Use the inverse CDF of the wind and load probability models to generate correlated wind and load forecast errors.
4. Calculate the net load errors by subtracting the wind errors from the load errors.
5. Determine an empirical CDF of the net load errors and determine the 5^{th} percentile of the negative net load errors.

We used an iterative process to determine the correct initial correlation of the variables in step one to create the proper level of correlation in the simulate error values. The simulated net load errors were used to calculate dispatchable generation capacity requirements for 95% day-ahead reliability. Figure 20 shows the results for a range of correlation coefficients with a load forecast near the mean forecast value and the wind forecast at the value of maximum uncertainty; 7,500 MW for ERCOT and 6,000 MW for MISO. Note that in figure 8 of the main text the amount of capacity required for 95% of day-ahead net load errors is 5,300 MW when forecasted wind is 7,500 MW in ERCOT and 3,100 MW when forecasted wind is 6,000 MW in MISO.

Wind forecast errors and load forecast errors have the opposite effect on net load forecast errors. For this reason, positively correlated wind and load forecast errors reduce net load uncertainty, while negatively correlated errors increase the uncertainty. As shown in figure 20, positive correlation reduces reserve requirements by up to 1050 MW in ERCOT and 700 MW in MISO. Negative correlation increases reserve requirements by up to 900 MW in ERCOT and 600 MW in MISO to cover 95% of day-ahead net load uncertainty.

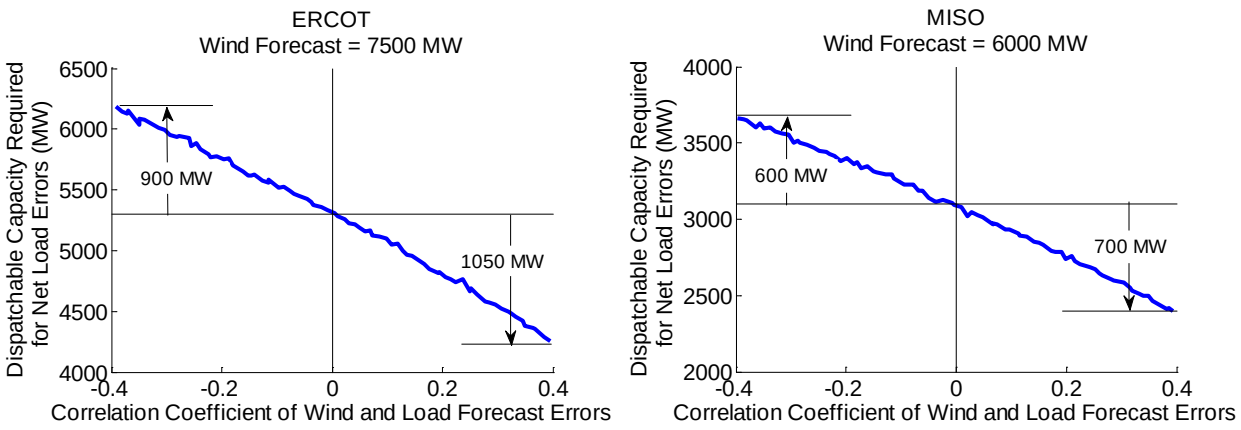

Figure 20: Dispatchable generation capacity required to cover net load forecast errors if wind and load forecasts are correlated. Load forecasts are between 90 and 120% of mean load and wind forecast is set such that wind uncertainty is at a maximum.

4. Look-ahead time effect on forecasts

Our treatment of load forecast errors combines load forecasts made for each hour of the day. The forecast is made once per day meaning that the look-ahead time is different for each hour. If the load forecast accuracy is greatly affected by the look-ahead time, then a better method would be to model load forecast errors by hour. Since we only have one forecast per day, it is not possible to observe the effects of look-ahead time on the load forecasts. Here we consider the effect of the look-ahead time by comparing forecast errors from the first (midnight to 1 a.m.) and last (11 p.m. to midnight) hours of each day on consecutive days. The errors come from two different forecasts. These errors are plotted against each other in figure 21 for ERCOT and MISO. We assume that load is very similar during these two hours. While this is not definitive, it shows evidence that the load level is more important than the look-ahead time.

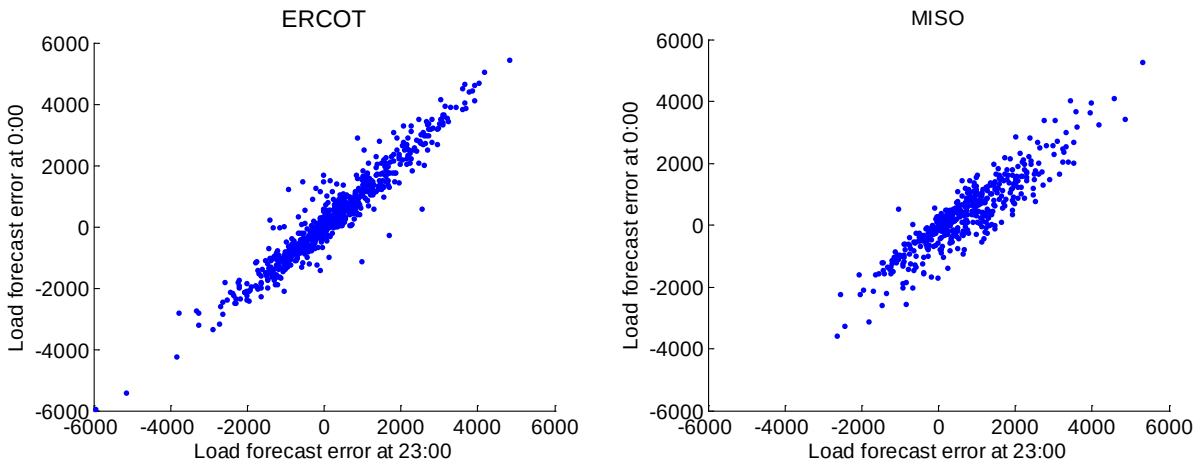

Figure 21: Load forecast errors for hour 1 and hour 24 on consecutive days made with different forecasts (two consecutive hours). The forecasts have very different look-ahead times but the errors are highly correlated.

Wind forecast uncertainty is obviously dependent on look-ahead time. However, for the time period used in day-ahead forecasts the uncertainty increases only a modest amount with look-ahead time. Figure 22 shows the root mean squared error for our ERCOT data set. Day-ahead forecasts used look-ahead times from 19 to 36 hours. The range of RMSE values as a fraction of installed wind capacity over these look-ahead times is 0.13 to 0.15.

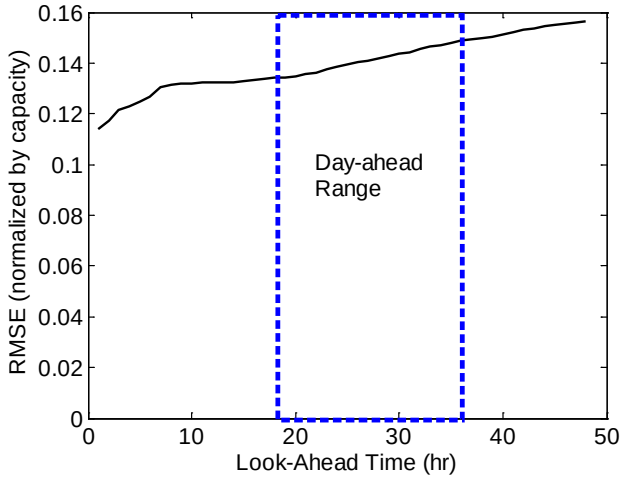

Figure 22: Wind forecast root mean squared error values in ERCOT for look-ahead times 1 to 48 hours. The day-ahead time frame is shown in the figure. RMSE is displayed as a fraction of installed wind capacity.

When looking at the RMSE value for different wind forecast levels, it becomes apparent that the wind forecast level has a much greater effect on uncertainty than the look-ahead time. Figure 23 shows the same data separated according the forecast level. Wind forecast errors were placed into four different bins: forecasts less than 20% of wind capacity, forecasts between 20% and 40% of wind capacity, forecasts between 40% and 60% capacity, and forecasts greater than 60% of wind capacity. RMSE values increase to a greater degree with forecast values compared with look-ahead time.

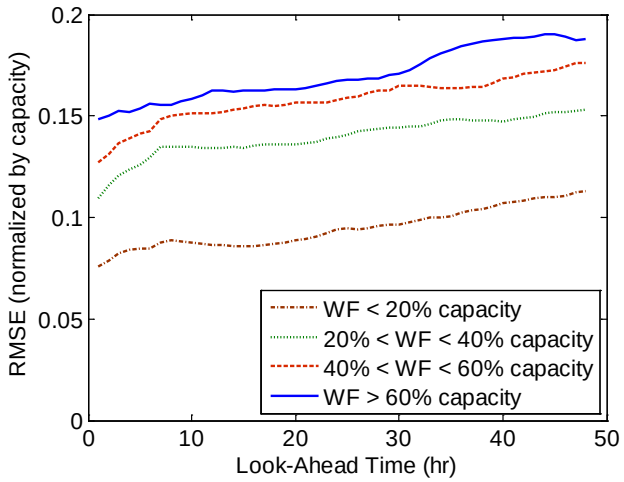

Figure 23: Wind forecast root mean squared error values in ERCOT for look-ahead times 1 to 48 hours with forecast errors are separated into four classes according to the forecast level. High forecasts are much more uncertain than low forecasts. RMSE is displayed as a fraction of installed wind capacity.